Journal of Magnetism and Magnetic Materials 320 (2008) L141–L143

Contents lists available at ScienceDirect

Journal of Magnetism and Magnetic Materials

journal homepage: www.elsevier.com/locate/jmmm

Letter to the Editor

Composition dependence of magnetic anisotropy and quadratic magnetooptical effect in epitaxial films of the Heusler alloy Co_2MnGe

P.K. Muduli, W.C. Rice, L. He, F. Tsui *

Department of Physics and Astronomy, University of North Carolina Chapel Hill, NC 27599, USA

ARTICLE INFO

Article history:
Received 5 November 2007
Available online 25 June 2008

Keywords:
Heusler alloy
Magnetic anisotropy
Magnetooptical effect

ABSTRACT

Magnetic anisotropy and magnetooptic Kerr effect for epitaxial films of $Co_xMn_yGe_{1-x-y}$ grown on Ge (111) substrates have been studied systematically in the compositional vicinity of the Heusler alloy Co_2MnGe. A large quadratic magnetooptic Kerr effect has been observed within a narrow region of composition centered around the Co to Mn atomic ratio of 2. The effect has been used to probe and quantify the magnetic anisotropy of the system, which is shown to have a strong sixfold in-plane component accompanied by a weak uniaxial component at room temperature. These properties are shown to depend sensitively on atomic ratio between Co and Mn, indicating the presence of an intrinsic composition-driven phenomenon.

Heusler alloys belong to an interesting class of ternary compounds that includes many predicted half-metals [1,2]. Their spin-dependent states and magnetism are expected to depend sensitively on stoichiometry, epitaxial constraints, and the presence of various structural and chemical disorders [3], but very little is known about these dependencies, owing primarily to the complexity associated with a ternary system and thus the difficulties for studying these. For example, dependence of magnetic anisotropy on stoichiometry is an important and yet relatively unexplored property, critical for understanding and controlling the magnetism in this important class of materials. Recent advances in combinatorial molecular-beam epitaxy (MBE) have made it possible to map the composition of an entire ternary system onto a single substrate and to explore the material system systematically [4]. In this paper, we report a systematic study of magnetic anisotropy and magnetooptic properties of a ternary system $Co_xMn_yGe_{1-x-y}$ in the compositional vicinity of the Heusler alloy Co_2MnGe, a predicted half-metal with a high Curie temperature [2].

The ternary combinatorial epitaxial film was grown by MBE techniques on a Ge (111) substrate at 250 °C and at a deposition rate of 0.1 Å/s to a nominal thickness of ~630 Å. A multilayer method was employed via sequential deposition of submonolayer "wedges" of the 3 elements [5]. The alloy film was subsequently annealed at 450 °C. The growth and annealing conditions were optimized for the best structural quality of the Heusler composition [6]. The ternary composition was examined and quantified using an array of complementary techniques, including X-ray fluorescence spectroscopy [7], secondary ion mass-spectrometry, electron energy dispersive X-ray spectroscopy, and Rutherford backscattering spectroscopy. In Fig. 1(a), a schematic diagram of the combinatorial sample is shown, indicating the ternary region (the triangle) and the location of Co_2MnGe. Structural investigations using regular and anomalous X-ray diffraction techniques [7,8] indicate that epitaxial films within this region of composition exhibit a high degree of structural and chemical ordering.

The magnetooptic Kerr effect (MOKE) measurements were performed at room temperature in the longitudinal geometry using a diode laser (wavelength of 664.3 nm). A standard lock-in technique with a photoelastic modulator was used for simultaneous detection of both Kerr rotation and ellipticity. The laser spot on the sample was focused to ~100 μm in diameter, which corresponds to ~1 at% in the composition space. The sample was mounted on a precision translation and rotation stage, and it was scanned with respect to the laser spot in order to probe the composition dependence. MOKE hysteresis loops were measured at each position with the magnetic field directed along more than 10 in-plane directions, including all of the in-plane ⟨110⟩ and ⟨112⟩ directions. Scribed crosshairs with line width of ~10 μm on the sample were used to position the laser spot on the sample, resulting in a positional reproducibility of better than 20 μm (~0.2 at% in composition) between different measurements.

MOKE hysteresis loops in the vicinity of Co_2MnGe exhibit a pronounced asymmetry with respect to the origin, as shown in Fig. 1(b) and (c). For example, as the Ge concentration increases through the Heusler stoichiometry, a characteristic "spike" emerges in the hysteresis loop near the positive coercive field (Fig. 1(c)); at a fixed Ge concentration, as the atomic ratio between Co and Mn passes through the value of 2, a reversal of the

* Corresponding author.
E-mail address: ftsui@physics.unc.edu (F. Tsui).

0304-8853/$ - see front matter © 2008 Elsevier B.V. All rights reserved.
doi:10.1016/j.jmmm.2008.06.027

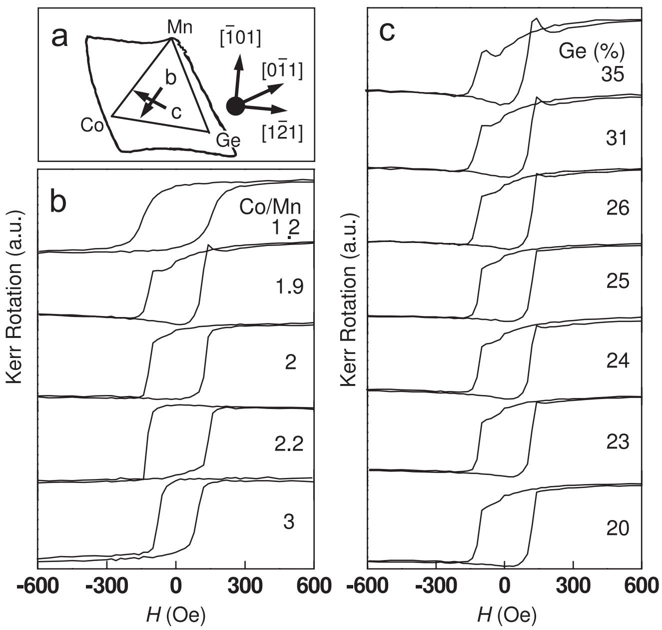

Fig. 1. (a) Schematic diagram of the sample under investigation showing the outline of the sample edges and the crystallographic directions with [111] pointing out of the page. The ternary region of composition is indicated by the triangle. The arrows within the triangle indicate the respective locations where the data shown in (b) and (c) were taken, and their intersection marks the Heusler stoichiometry. (b) and (c) Evolution of MOKE hysteresis loops as a function of composition: (b) changing atomic ratio Co/Mn at a fixed Ge concentration of 25 at%, and (c) changing Ge concentration (in at%) at a fixed Co/Mn atomic ratio of 2. The MOKE hysteresis loops are measured with H directed 75° from [0 $\bar{1}$ 1], i.e. between [$\bar{1}$ 0 1] and [$\bar{2}$ 1 1], and with an incidence angle for the laser ~10°.

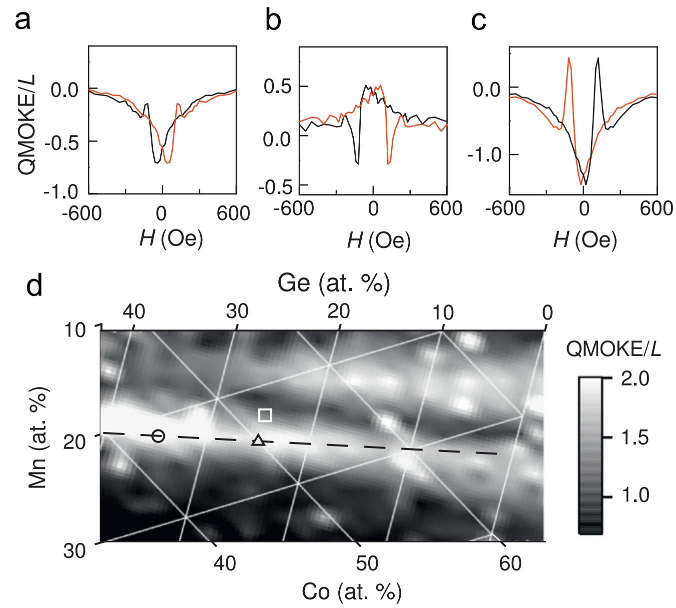

Fig. 2. (Color online) Normalized QMOKE loops (QMOKE/L) versus composition for $Co_xMn_yGe_z$ with H directed 75° from [0 $\bar{1}$ 1]: (a) $x/y = 2$ and $z = 25$ at%, (b) $x/y = 2.2$ and $z = 25$ at%, and (c) $x/y = 2$ and $z = 35$ at%. The black and red lines correspond to $H_\downarrow$ and $H_\uparrow$, respectively. (d) Maximum amplitude of QMOKE/L versus composition for $H \parallel$ [1 $\bar{2}$ 1] and an angle of incidence for the laser ~6°. The symbols, triangle, square and circle correspond to the composition for (a), (b) and (c), respectively.

hysteresis asymmetry occurs (Fig. 1(b)). The observed asymmetry is a result of a strong second-order or quadratic magnetooptic Kerr effect (QMOKE) that arises from higher order spin-orbit interactions [9,10]. The consequence is that both magnetization projections parallel and perpendicular to the field, $M_\parallel$ and $M_\perp$, respectively, are detected by MOKE. For instance, a sudden jump in magnetization direction can produce a "spike" in the hysteresis loop.

To the second order of saturation magnetization M_s, the measured Kerr rotation, $\phi_K(H_{\uparrow\downarrow})$ can be expressed as

$$LM_\parallel + Q_0 M_\parallel M_\perp + Q_1(M_\parallel^2 - M_\perp^2). \quad (1)$$

Here, L is the coefficient for the linear MOKE (LMOKE), and Q_0 and Q_1 are those for QMOKE, and the arrows in the subscript indicate the sweep directions of the field H. The coefficients depend on the MOKE geometry and the off-diagonal elements of the dielectric tensor [9,10]. The symmetry of Eq. (1) allows the measured MOKE hysteresis loops $\phi_K(H_{\uparrow\downarrow})$ to be separated into

$$\mathrm{LMOKE}_{\uparrow\downarrow} = [\phi_K(H_{\uparrow\downarrow}) - \phi'_K(H_{\downarrow\uparrow})]/2 \text{ and}$$
$$\mathrm{QMOKE}_{\uparrow\downarrow} = [\phi_K(H_{\uparrow\downarrow}) + \phi'_K(H_{\downarrow\uparrow})]/2,$$
$$\text{where } \phi'_K(H_{\downarrow\uparrow}) \text{ is} \quad (2)$$

the inversion of $\phi_K(H_{\uparrow\downarrow})$ with respect to H, i.e. $\phi'_K(H_{\uparrow\downarrow}) = \phi_K(-H_{\uparrow\downarrow})$.

The hysteresis loops of QMOKE have been normalized by the corresponding saturation values of LMOKE [11], L, and as shown in Fig. 2, the normalized loops (QMOKE/L) have different shapes and large amplitudes in the compositional vicinity of the Heusler stoichiometry. For a light incident angle of $<6°$, the observed QMOKE amplitudes exhibit a narrow ridge (values >1 and as high as 2.5) along the Co to Mn atomic ratio of 2 (Fig. 2(d)). This narrow region of large QMOKE values appears to coincide with the region where a high degree of structural and chemical ordering has been observed [8]. The QMOKE values reported here are comparable to previously reported values for Heusler alloys of Co_2FeSi [11] and PtMnSb [12]. Since large QMOKE values enhance the sensitivity for detecting and quantifying magnetization directions (Eq. (1)), the effect has been used to analyze the magnetic anisotropy of the system, as discussed below.

The measured MOKE hysteresis loops as a function of field directions have been simulated using Eq. (1). The magnetization directions, on the other hand, have been calculated using a single domain Stoner–Wohlfarth model [13,14] by minimizing the energy density associated with the in-plane magnetic anisotropy, E_{IPMA}. For the (111) symmetry, the energy density is given by

$$E_{\mathrm{IPMA}} = K_6(28 - \cos 6\theta)/108 + K_u \sin^2(\theta - \varphi) - M_\parallel H. \quad (3)$$

Here, the sixfold magnetic anisotropy with the corresponding constant K_6 (the first term) arises from crystal symmetry in thin-film geometry, with θ being the angle between the direction of magnetization and one of the sixfold easy axes (for $K_6 > 0$). A uniaxial correction (K_u) is added (the second term) with φ the angle between the uniaxial easy axis and one of the sixfold easy axes. The last term represents the Zeeman energy.

The model simulations, as described above using K_6/M_s, K_u/M_s, Q_0/L, and Q_1/L as the adjustable parameters, have yielded good qualitative agreements with the measured hysteresis loops, as shown in Fig. 3 for a typical set with $K_6/M_s = (1200 \pm 100)$ Oe and $K_u/M_s = (20 \pm 3)$ Oe. The sixfold easy axes are determined to be along the in-plane ⟨110⟩ directions consistent with the crystal symmetry. A weak uniaxial magnetic anisotropy (UMA) is often needed in order to produce the distinct features in the hysteresis loops, and near the Heusler stoichiometry, the easy axis for UMA is near [0 $\bar{1}$ 1]. We note that the observed magnetooptical parameters at a single composition depend on the geometries of the measurement. Specifically, the parameters Q_0 and Q_1 exhibit a monotonic increase with decreasing incident angle, while the counterpart L exhibits a corresponding decrease [9,10,15]. In addition, a second-order magnetization-induced

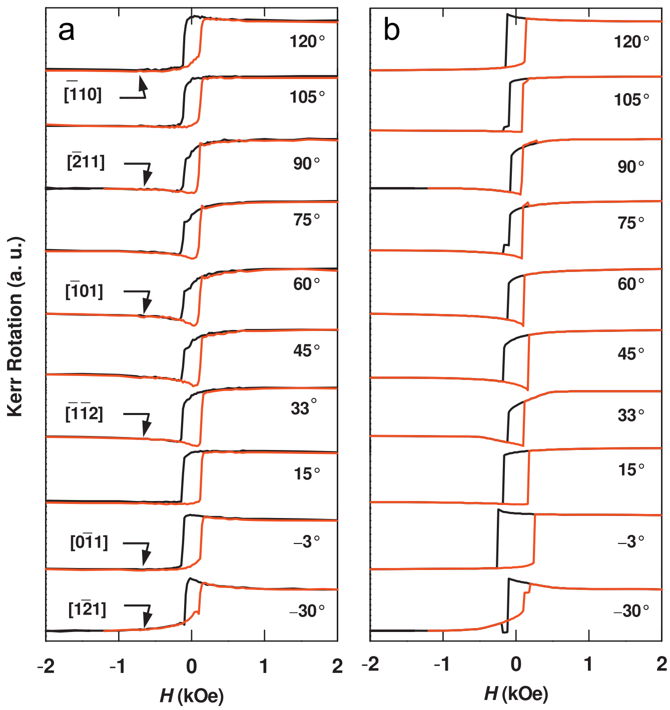

Fig. 3. (Color online) Comparison between the measured angle-dependent MOKE hysteresis loops (a) and the simulation (b) for Co_2MnGe. The black and red lines correspond to $H_\downarrow$ and $H_\uparrow$, respectively. The listed angles are measured from the in-plane [0 1̄ 1]. Angle of incidence for the laser is ~10°.

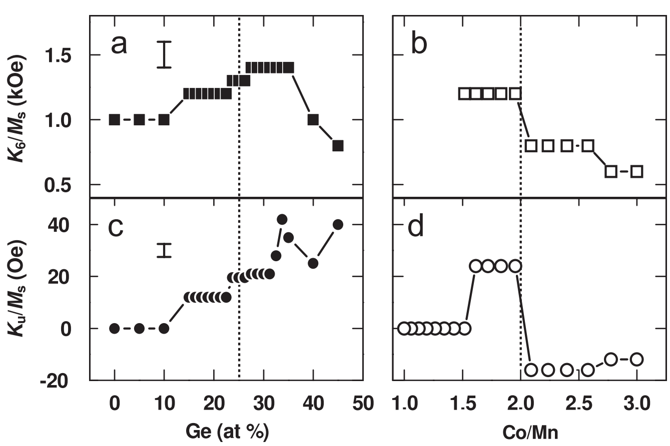

Fig. 4. Evolution of magnetic anisotropy constants as a function of composition: (a) and (b) K_6/M_s, and (c) and (d) K_u/M_s. Error bars for the respective constants are shown in (a) and (c). Dependence on Ge concentration at a fixed Co/Mn ratio of 2 is shown in (a) and (c), whereas the behavior for a fixed Ge concentration of 25 at% is shown in (b) and (d). The dotted lines indicate the location of Heusler stoichiometry.

optical anisotropy with respect to the in-plane field directions (expected theoretically from the crystal symmetry [16]) is also observed, and thus included in the analysis (Fig. 3). These effects, however, are not the focus of this letter, and they will be discussed elsewhere [15].

Quantitative values of magnetic anisotropy as a function of composition have been obtained from the analysis. They exhibit a relatively narrow ridge along a constant Co to Mn atomic ratio of 2 that correlates with the one for QMOKE (Fig. 2). The behaviors along and across the ridge are shown, respectively, in the left and right column of Fig. 4. On the ridge, the values for the sixfold anisotropy are very large, exhibiting a broad peak near Ge concentration of 30 at% (Fig. 4(a)), while the UMA counterparts are very small and increase with Ge concentration (Fig. 4(c)). Near the Heusler stoichiometry, K_6 is determined to be $(1.2\pm0.2)\times10^6$ ergs/cm^3 using the bulk M_s [17]. Across the ridge, as the Co/Mn ratio exceeds 2, the anisotropy values change abruptly, and in particular the UMA exhibits a sign change (Fig. 4(d)) that corresponds to a 90° reorientation of the UMA easy axis. As the atomic ratio decreases from 2, a transition from anisotropic to isotropic behavior takes place near Co/Mn of 1.5 (Fig. 4(b) and (d)). The latter transition correlates with a first-order structural phase transition from cubic to hexagonal [7]. In the isotropic region the hysteresis loops exhibit a large switching width (Fig. 1(b)) with no quadratic effect.

While there are various extrinsic sources and interactions that affect the nature and strength of magnetic anisotropy and magnetooptical effect for any given sample, the observed composition dependence, particularly the symmetry and sensitivity on the Co to Mn atomic ratio, strongly support the presence of an intrinsic composition driven phenomenon. Such a phenomenon is not previously known for any Heusler alloys, and it appears to be responsible for the observed ordering around Co/Mn ratio of 2 and for the observed strong correlation and interplay between structure, magnetism, and magnetooptical effects. Since both magnetic anisotropy and magnetooptical effects, in particular QMOKE, are the result of corresponding spin-orbit interactions, the electronic structure of the system and perhaps chemical ordering within the lattice may also be driven by the same composition dependent phenomenon. These findings should provide the necessary impetus for future work in this material system in order to elucidate the origin of the composition driven effect and to control magnetism and spin-dependent states. From a broader perspective, while properties of complex alloys are generally expected to depend on composition, investigations into how the dependence takes place should still take precedence.

The authors wish to thank B. A. Collins for carrying out structural analysis using X-ray techniques and for discussion. The work is supported by DOE BES DE-FG02-05ER46216. MBE synthesis is supported by NSF DMR-0441218.

References

[1] R.A. de Groot, F.M. Mueller, P.G. van Engen, K.H.J. Buschow, Phys. Rev. Lett. 50 (1983) 2024.
[2] S. Ishida, T. Masaki, S. Fujii, S. Asano, Physica B 245 (1998) 1; S. Ishida, S. Fujii, H. Nagayoshi, S. Asano, Physica B 254 (1998) 157.
[3] S. Picozzi, A. Continenza, A.J. Freeman, Phys. Rev. B 69 (2004) 094423.
[4] Y.K. Yoo, F. Tsui, MRS Bull. 27 (2002) 316.
[5] F. Tsui, L. He, Rev. Sci. Instrum. 76 (2005) 062206.
[6] F. Tsui, L. He, L. Ma, Mater Res. Soc. Symp. Proc. vol. 700, Warrendale, PA, Materials Research Society, 2002, S2.2.
[7] F. Tsui, L. He, D. Lorang, A. Fuller, Y.S. Chu, A. Tkachuk, S. Vogt, Appl. Surf. Sci. 252 (2006) 2512 (and references therein).
[8] B.A. Collins, Y. Zhong, Y.S. Chu, L. He, F. Tsui, J. Vac. Sci. Technol. B 25 (2007) 999.
[9] R.M. Osgood III, B.M. Clemens, R.L. White, Phys. Rev. B 55 (1997) 8990.
[10] K. Postava, H. Jaffres, A. Schuhl, F. Nguyen Van Dau, M. Goiran, A.R. Fert, J. Magn. Magn. Mater. 172 (1997) 199.
[11] J. Hamrle, S. Blomeier, O. Gaier, B. Hillebrands, H. Schneider, G. Jakob, K. Postava, C. Felser, J. Phys. D 40 (2007) 1563.
[12] R. Carey, D.M. Newman, M.L. Wears, Phys. Rev. B 58 (1998) 14175.
[13] E.C. Stoner, E.P. Wohlfarth, Philos. Trans. R. Soc. London A 240 (1948) 74.
[14] J.M. Florczak, E.D. Dahlberg, Phys. Rev. B 44 (1991) 9338.
[15] P.K. Muduli, W.C. Rice, L. He, B.A. Collins, Y.S. Chu, F. Tsui, unpublished.
[16] K. Postava, D. Hrabovský, J. Pištora, A.R. Fert, Š. Višňovský, T. Yamaguchi, J. Appl. Phys. 91 (2002) 7293.
[17] P.J. Webster, J. Phys. Chem. Solids 32 (1971) 1221.